Multistep Kinetic Behavior of the Thermal Decomposition of Granular Sodium Percarbonate: Hindrance Effect of the Outer Surface Layer

Takeshi Wada, Masayoshi Nakano, and Nobuyoshi Koga*

Chemistry Laboratory, Department of Science Education, Graduate School of Education, Hiroshima University, 1-1-1 Kagamiyama, Higashi-Hiroshima 739-8524, Japan

S1. Sample Characterization

The major XRD peaks of the as-received SPC granules (Figure S1) were indexed to those of $Na_2CO_3 \cdot 1.5H_2O_2$ (orthorhombic, S.G.: *Cmca*, a = 6.7138Å, b = 15.7407Å, c = 9.1732Å, JCPDS 11-0656),[S1] but some minor peaks were also detected. After exposing the SPC granules in air for several months, those minor peaks substantially grew (Figure S2) and were clearly assigned to those of $Na_2CO_3 \cdot H_2O$ (orthorhombic, S.G.: *Pca21*, a = 10.72 Å, b = 5.249 Å, c = 6.469 Å, JCPDS 8-0448). The minor phase of $Na_2CO_3 \cdot H_2O$ in the as-received SPC granules was likely generated during the granulation process via the decomposition of SPC and is a component in the outer surface layer of the granules. The FT-IR spectrum of the as-received SPC granules (Figure S3) was in agreement with that reported previously for SPC crystalline particles and included IR absorption peaks attributed to H_2O_2 and CO_3^{2-}: symmetric O–H stretching (3040 cm^{-1}); asymmetric O–H stretching (2359 cm^{-1}); H_2O_2 deformation (1559 cm^{-1}); O–O stretching (856 cm^{-1}); H_2O_2 torsion (959 cm^{-1}); and internal CO_3^{2-} modes (1437 and 698 cm^{-1}).[S2,S3]

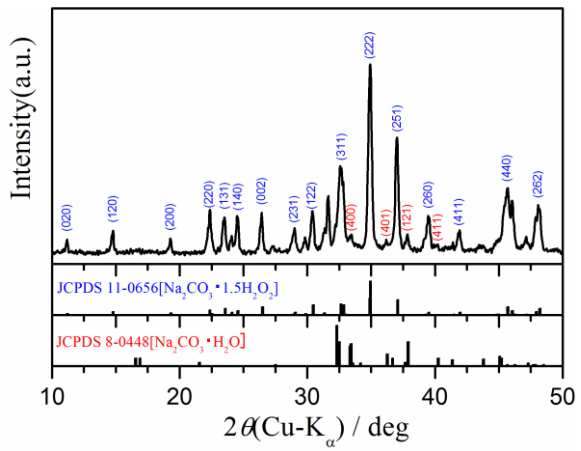

Figure S1. XRD pattern of the as-received SPC granules.

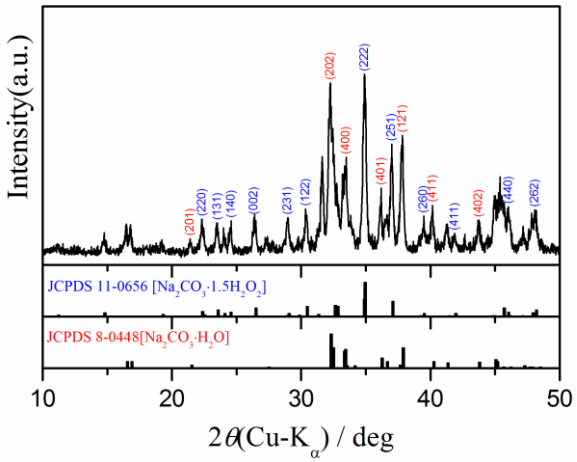

Figure S2. XRD pattern of the partially hydrated SPC granules.

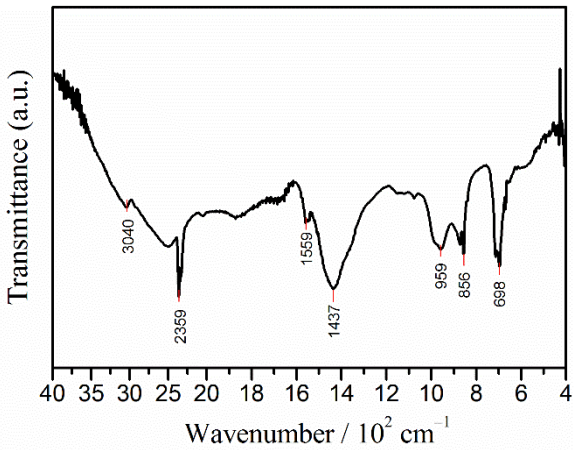

Figure S3. FT-IR spectrum of the as-received SPC granules.

S2. Overview of the Thermal Decomposition Process

Upon heating the crushed SPC granules according to a stepwise isothermal heating program (300 to 525 K) in flowing N_2, the XRD pattern for $Na_2CO_3 \cdot 1.5H_2O_2$ changed to Na_2CO_3 (monoclinic b axis, S.G.: C*/*, a = 8.907 Å, b = 5.239 Å, c = 6.043 Å, β = 101.3°, JCPDS

* Correspondence author: e-mail nkoga@hiroshima-u.ac.jp.

19-1130) in the temperature range from 375 to 425 K (Figure S4). No other crystalline phases of intermediate compounds were detected during the thermal decomposition.

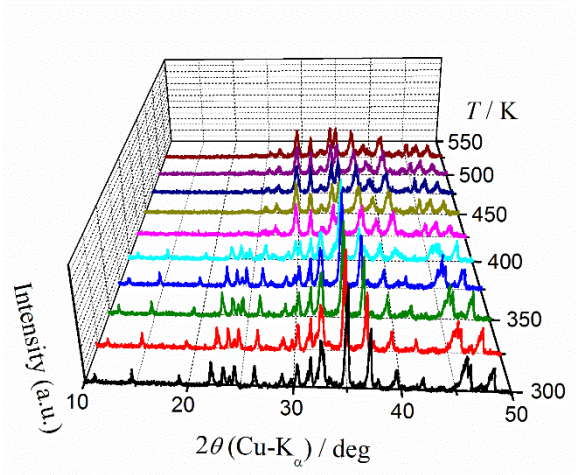

Figure S4. Changes in the XRD pattern of crushed SPC granules during stepwise isothermal heating in flowing N_2 (100 cm^3 min^{-1}).

S3. Kinetic Analysis using a Mathematical Peak Deconvolution Procedure

The DTG curve for the thermal decomposition of SPC granules recorded under linear nonisothermal conditions (Figure S5) was separated into two partially overlapping peaks with satisfactory fit using Weibull functions:[S4-S6]

$$y = \left[\begin{array}{l} a_0 \left(\dfrac{a_3 - 1}{a_3} \right)^{\frac{1-a_3}{a_3}} \left\{ \dfrac{x - a_1}{a_2} + \left(\dfrac{a_3 - 1}{a_3} \right)^{\frac{1}{a_3}} \right\}^{a_3 - 1} \\ \exp\left[- \left\{ \dfrac{x - a_1}{a_2} + \left(\dfrac{a_3 - 1}{a_3} \right)^{\frac{1}{a_3}} \right\}^{a_3} + \dfrac{a_3 - 1}{a_3} \right] \end{array} \right]. \qquad \text{(S1)}$$

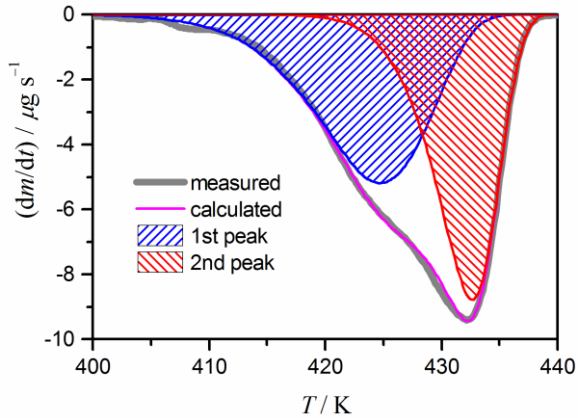

Figure S5. Typical mathematical deconvolution of the DTG curve for the thermal decomposition of SPC granules at β = 5 K min^{-1} using Weibull functions.

From the ratio of the peak areas for the separated first and second peaks, the contribution c of each peak to the overall reaction was determined as (c_1, c_2) = (0.52 ± 0.02, 0.48 ± 0.02). The mathematically separated peaks at different β were used as the kinetic rate data (Figure S6).

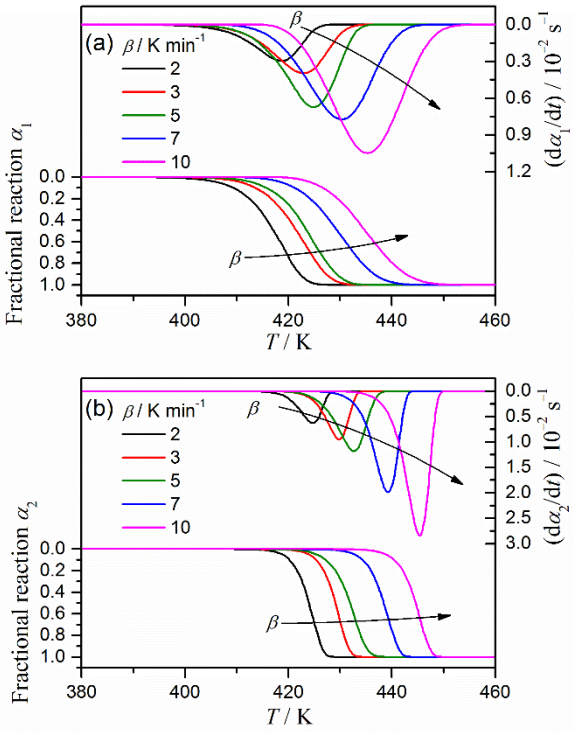

Figure S6. Kinetic rate data at different β derived from the mathematically separated DTG peaks: (a) first peak (i = 1) and (b) second peak (i = 2).

For both the first and second peaks, the kinetic rate data indicated systematic shifts to higher temperatures with increasing β. On the other hand, very different trends for the α-dependent changes in the apparent activation energies (E_a) determined by applying the Friedman method[S7] were found for the kinetic rate data of the separated first and second DTG peaks (Figure S7). For the first DTG peak, a systematic decrease in the E_a value during the course of the reaction was observed, while for the second DTG peak, a practically constant E_a value was obtained. The systematic change in the E_a value with α observed for the first peak indicates that the isoconversional relationship failed because of the changes in the self-generated conditions as the reaction advanced and depending on β. In this situation, an average value for $E_{a,1}$, 109.1 ± 20.8 kJ mol^{-1} ($0.1 \leq \alpha_1 \leq 0.9$), was tentatively used as the E_a value for the first peak. The average value for the practically constant $E_{a,2}$ value for the second peak was 115.5 ± 1.3 kJ mol^{-1} ($0.05 \leq \alpha_2 \leq 0.95$). These E_a values are nearly coincident with one another and also in agreement with that determined for the overall reaction under isothermal and controlled rate conditions, 112.5 ± 1.2 kJ mol^{-1} ($0.05 \leq \alpha \leq 0.95$).

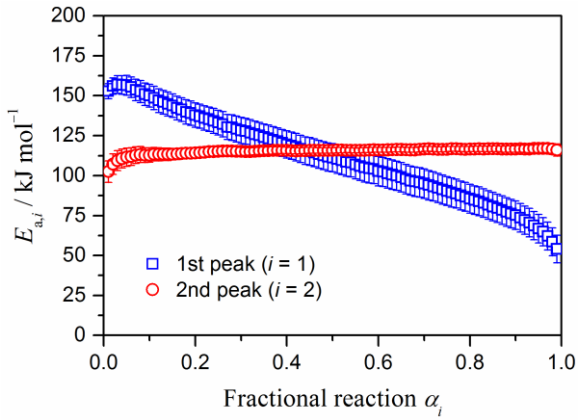

Figure S7. E_a values at different α determined using the Friedman method for the separated first and second DTG peaks.

Using the respective E_a values, experimental master plots of $(d\alpha/d\theta)$ versus α[S8-S14] for the separated first and second DTG peaks were drawn (Figure S8) and satisfactorily fitted using the JMA(m) model[S15-S18] with $m_1 = 2.15 \pm 0.01$ and $m_2 = 5.80 \pm 0.01$, respectively. The values for the preexponential factor A for the first and second peaks determined through nonlinear regression analysis for the fitting using the JMA(m) model were $A_1 = (3.22 \pm 0.01) \times 10^{11}$ s^{-1} and $A_2 = (4.83 \pm 0.01) \times 10^{11}$ s^{-1}, respectively.

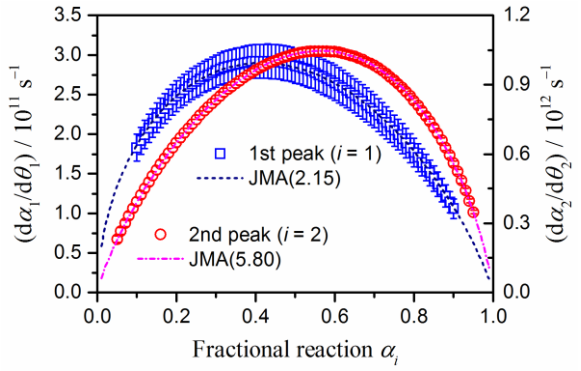

Figure S8. Experimental master plots of $(d\alpha/d\theta)$ versus α for the separated first and second DTG peaks and fitting curves obtained using the JMA(m) model.

S4. Initial Kinetic Parameters for the Kinetic Deconvolution

The initial c_i values for the reaction under linear nonisothermal conditions were taken from those determined by the mathematical deconvolution. Because of the systematic decrease in the $E_{a,1}$ values determined for the first DTG peak (Figure S7), the average E_a value determined for each separated peak was not employed for the initial values. Instead, considering the close agreement of both average $E_{a,i}$ values for the separated DTG peaks with that determined for the reaction under isothermal and controlled conditions, the latter value of 112.5 kJ mol^{-1} was adopted for both reaction steps. The kinetic exponents m in the JMA(m) model for each reaction step were set to 3.00 with expecting variation to a suitable value through the subsequent optimization run. After setting these kinetic parameters in Eq. 8 (see the main text), the order of the A_i values for each reaction step was determined by graphically comparing the result to the experimental kinetic curve. Table S1 summarizes the initial kinetic parameters used for the kinetic deconvolution analysis for the reaction under linear nonisothermal conditions.

Table S1. Initial kinetic parameters used for the kinetic deconvolution analysis of the thermal decomposition of SPC granules under linear nonisothermal conditions

Peak i	c_i	$E_{a,i}$ / kJ mol^{-1}	m_i in JMA(m)	A_i / s^{-1}
1	0.52	112.5	3.00	6.0×10^{11}
2	0.48	112.5	3.00	3.0×10^{11}

References

(S1) Pritchard, R. G.; Islam, E., Sodium Percarbonate between 293 and 100 K. *Acta Crystallogr., Sect. B* **2003**, *59*, 596-605.

(S2) Wada, T.; Koga, N., Kinetics and Mechanism of the Thermal Decomposition of Sodium Percarbonate: Role of the Surface Product Layer. *J. Phys. Chem. A* **2013**, *117*, 1880-1889.

(S3) de C. T. Carrondo, M. A. A. F.; Griffith, W. P.; Jones, D. P.; Skapski, A. C., X-Ray Crystal Structure of the Industrial Bleaching Agent 'Sodium Percarbonate'[Sodium Carbonate-Hydrogen Peroxide (2/3)]. *J. Chem. Soc., Dalton Trans.* **1977**, 2323-2327.

(S4) Cai, J.; Liu, R., Weibull Mixture Model for Modeling Nonisothermal Kinetics of Thermally Stimulated Solid-State Reactions: Application to Simulated and Real Kinetic Conversion Data. *J. Phys. Chem. B* **2007**, *111*, 10681-10686.

(S5) Perejon, A.; Sanchez-Jimenez, P. E.; Criado, J. M.; Perez-Maqueda, L. A., Kinetic Analysis of Complex Solid-State Reactions. A New Deconvolution Procedure. *J. Phys. Chem. B* **2011**, *115*, 1780-1791.

(S6) Koga, N.; Goshi, Y.; Yamada, S.; Pérez-Maqueda, L. A., Kinetic Approach to Partially Overlapped Thermal Decomposition Processes. *J. Therm. Anal. Calorim.* **2013**, *111*, 1463-1474.

(S7) Friedman, H. L., Kinetics of Thermal Degradation of Cha-Forming Plastics from Thermogravimetry, Application to a Phenolic Plastic. *J. Polym. Sci., Part C* **1964**, *6*, 183-195.

(S8) Ozawa, T., A New Method of Analyzing Thermogravimetric Data. *Bull. Chem. Soc. Jpn.* **1965**, *38*, 1881-1886.

(S9) Ozawa, T., Kinetic Analysis of Derivative Curves in Thermal Analysis. *J. Therm. Anal.* **1970**, *2*, 301-324.

(S10) Ozawa, T., Applicability of Friedman Plot. *J. Therm. Anal.* **1986**, *31*, 547-551.

(S11) Málek, J., A Computer Program for Kinetic Analysis of Non-Isothermal Thermoanalytical Data. *Thermochim. Acta* **1989**, *138*, 337-346.

(S12) Málek, J., The Kinetic Analysis of Non-Isothermal Data. *Thermochim. Acta* **1992**, *200*, 257-269.

(S13) Koga, N., Kinetic Analysis of Thermoanalytical Data by Extrapolating to Infinite Temperature. *Thermochim. Acta* **1995**, *258*, 145-159.

(S14) Gotor, F. J.; Criado, J. M.; Malek, J.; Koga, N., Kinetic Analysis of Solid-State Reactions: The Universality of Master Plots for Analyzing Isothermal and Nonisothermal Experiments. *J.Phys. Chem. A* **2000**, *104*, 10777-10782.

(S15) Avrami, M., Kinetics of Phase Change. I. General Theory. *J. Chem. Phys.* **1939**, *7*, 1103-1112.
(S16) Avrami, M., Kinetics of Phase Change. II. Transformation-Time Relations for Random Distribution of Nuclei. *J. Chem. Phys.* **1940**, *8*, 212-223.
(S17) Avrami, M., Kinetics of Phase Change. III. Granulation, Phase Change, and Microstructure. *J. Chem. Phys.* **1941**, *9*, 177-184.
(S18) Barmak, K., A Commentary On: "Reaction Kinetics in Processes of Nucleation and Growth". *Metall. Mater. Trans. A* **2010**, *41*, 2711-2775.